

**Urotensin II induces rat cardiomyocyte hypertrophy *via* the transient oxidization of Src homology 2-containing tyrosine phosphatase and transactivation of epidermal growth factor receptor**

Ju-Chi Liu, Cheng-Hsien Chen, Jin-Jer Chen, and Tzu-Hung Cheng

Department of Medicine, Taipei Medical University-Shuang Ho Hospital, Taipei, Taiwan, R.O.C. (J.-C. L., C.-H. C.); Department of Internal Medicine, National Taiwan University Hospital and National Taiwan University College of Medicine, Taipei, Taiwan, R.O.C. (J.-J. C.); Department of Biological Science and Technology, College of Life Sciences, China Medical University, Taichung, Taiwan, R.O.C. (T.-H. C.).

Running Title: Urotensin II induces rat cardiomyocyte hypertrophy

Address correspondence to:

Dr. Tzu-Hung Cheng,

Department of Biological Science and Technology, College of Life Sciences, China  
Medical University, Taichung, Taiwan, R.O.C.

No.91 Hsueh-Shih Road, Taichung, Taiwan 40402, R.O.C.

E-mail:thcheng@mail.cmu.edu.tw

Number of text pages: 31.

Number of tables: 0.

Number of figures: 7.

Number of references: 20.

Number of words in the Abstract: 245.

Number of words in the Introduction: 519.

Number of words in the Discussion: 984.

**Abbreviations:** U-II, urotensin II; EGFR, epidermal growth factor receptor; ROS, reactive oxygen species; *N*-acetyl cysteine, NAC; SHP-2, Src homology 2-containing tyrosine phosphatase; PTP 1B, protein tyrosine phosphatase 1B; ERK, extracellular signal-regulated kinase; DMEM, Dulbecco's modified Eagle's medium; DAPI, 4',6-diamidino-2-phenylindole; PBS, phosphate-buffered saline; DCFH, 2',7'-dichlorodihydrofluorescein; DCF, 2',7'-dichlorofluorescein; IAA, iodoacetic acid; GFP, green fluorescent protein.

## Abstract

Urotensin II (U-II) is implicated in cardiomyocyte hypertrophy, which results in cardiac remodeling. We recently demonstrated that both reactive oxygen species (ROS) generation and epidermal growth factor receptor (EGFR) transactivation play critical roles in U-II signal transduction. However, the detailed intracellular mechanism(s) underlying cardiac hypertrophy and remodeling remain unclear. In this study, we used rat cardiomyocytes treated with U-II to investigate the association between ROS generation and EGFR transactivation. U-II treatment was found to stimulate cardiomyocyte hypertrophy through phosphorylation of EGFR and ROS generation. Apocynin, an NAD(P)H oxidase inhibitor, and the ROS scavenger *N*-acetyl cysteine (NAC), both inhibited EGFR transactivation induced by U-II. In contrast, AG-1478 (an EGFR inhibitor) failed to inhibit intracellular ROS generation induced by U-II. Src homology 2-containing tyrosine phosphatase (SHP-2), but not protein tyrosine phosphatase 1B (PTP 1B), was shown to be associated with EGFR during U-II treatment by EGFR co-immunoprecipitation. ROS have been reported to transiently oxidize the catalytic cysteine of phosphotyrosine phosphatases, subsequently inhibiting their activity. We examined the effect of U-II on SHP-2 and PTP 1B in cardiomyocytes using a modified malachite green phosphatase assay. SHP-2, but not PTP 1B, was transiently oxidized during U-II treatment, which could be repressed by NAC treatment. In SHP-2 knockdown cells, U-II-induced phosphorylation of EGFR and myocyte hypertrophy were dramatically elevated, and these effects were not influenced by NAC. Our data suggest that U-II-mediated ROS generation can transiently inhibit SHP-2 activity, thereby facilitating EGFR transactivation and hypertrophic signal transduction in rat

MOL #58297

4

cardiomyocytes.

## Introduction

Cardiac remodeling is generally considered as a process occurring in response to increased cardiac load, which may be due to hypertension or neurohormonal elevations, injuries or other factors (Ni et al., 2006). Following adverse physiologic events, the heart undergoes compensatory changes in cardiac output that is necessary to maintain blood flow in the pulmonary and systemic circulation. These adaptive changes involve cardiac hypertrophy and, proliferation of cardiac fibroblasts, accompanied by simultaneous adjustments in the interstitial tissue. In the long-term, however, these modifications are highly detrimental and contribute to the subsequent inability of the cardiac system to maintain sufficient output, ultimately resulting in heart failure. Thus, in addition to representing a pathologic state that precedes cardiac failure, cardiac hypertrophy is also an independent risk factor for cardiac-related morbidity and mortality. Therefore, it is of particular importance to determine the molecular mechanisms underlying development of cardiac hypertrophy.

With regard to cardiovascular disease, there has been considerable interest in urotensin II (U-II) due to accumulating evidence suggesting it has a role in cardiac remodeling and subsequent cardiovascular dysfunction. U-II is a cyclic peptide synthesized through proteolytic cleavage of a precursor molecule, prepro-U-II, and is a potent vasoconstrictor (Saffitz et al., 2007). U-II has been identified in the heart (Matsushita et al., 2003), which is also known to display an abundant expression of U-II receptors (Saffitz et al., 2007). It is now well-established that U-II levels are significantly increased in several cardiovascular diseases (Bousette and Giaid, 2006). For example, in patients with coronary artery disease, it has been shown that U-II plasma levels are

significantly greater relative to normal patients. The severity of coronary artery disease is also positively correlated with U-II plasma levels (Papadopoulos et al., 2008). In addition to clinical evidence, *in vitro* and *in vivo* studies have further implicated U-II in the development of cardiac hypertrophy (Zhang et al., 2007). We recently demonstrated that generation of reactive oxygen species (ROS) is involved in U-II-induced cell proliferation, tyrosine phosphorylation of epidermal growth factor receptors (EGFRs), and extracellular signal-regulated kinase (ERK) phosphorylation in rat cardiac fibroblasts (Chen et al., 2008). However, little is known about U-II-mediated intracellular signaling pathways related to cardiomyocyte hypertrophy.

Although EGFR transactivation and ROS generation have important roles in U-II signaling pathways (Chen et al., 2008), the connection between these biochemical processes remains unclear. Recent studies have revealed a mechanism through which ROS can regulate cellular processes. This involves transient inhibition of protein tyrosine phosphatases (PTPs) through reversible oxidation of their catalytic cysteine residue, which in turn suppresses dephosphorylation of downstream proteins (Meng et al., 2002). Several PTPs regulate receptor tyrosine kinases associated with various signaling pathways, including EGFRs (Liebmann and Bohmer, 2000). This reversible oxidation mechanism may help to explain the link between EGFR transactivation and ROS generation in the U-II signaling pathway. Therefore, we examined the EGFR as a potential downstream effector of U-II-induced hypertrophy in neonatal rat cardiomyocytes. Here, we report that ROS generation is involved in EGFR transactivation and myocyte hypertrophy triggered by the U-II signaling pathway in rat cardiomyocytes. This mechanism is associated with transient inhibition of the PTP,

MOL #58297

7

SHP-2, caused by ROS.

## Materials and Methods

**Materials** Dulbecco's modified Eagle's medium (DMEM), fetal calf serum, and tissue culture reagents were obtained from Invitrogen (Carlsbad, CA). Human urotensin II (U-II) and all other chemicals of reagent grade were obtained from Sigma-Aldrich (St. Louis, MO). To block EGFR-mediated signaling or U-II induced ROS generation, cells were preincubated for 30 min at 37 °C with 4-(3-Chloroanilino)-6,7-dimethoxyquinazoline (AG1478), *N*-acetyl-cysteine (NAC), or apocynin prior to incubation with U-II. Antibodies used in this study were purchased from New England Biolabs (Beverly, MA), Cell Signaling Technology Inc. (Danvers, MA), BD Laboratories (San Diego, CA), Santa Cruz Biotechnology (Santa Cruz, CA), and Lab Frontier Co. Ltd. (anti-GAPDH) (Seoul, Korea).

**Cardiomyocyte cell culture and immunofluorescence microscopy** Primary cultures of neonatal rat ventricular myocytes were prepared and plated at high density (1250 cells/mm<sup>2</sup>) as previously described (Cheng et al., 1999). Principle of laboratory animal care" (NIH publication No. 86--23, revised 1985) were followed. Primary myocyte cell cultures contained less than 5 % non-cardiomyocytes as determined microscopically. Before treatment, serum-containing medium was removed from myocyte cultures and replaced with serum-free medium. In order to visualize changes in cell size, myocytes were plated on fibronectin-coated coverslips, at a density of  $5 \times 10^5$  cells in 35-mm dishes. After the treatment, cells were fixed and visualized using mouse anti- $\alpha$ -actinin (Sigma-Aldrich) and rhodamine-conjugated anti-mouse antibodies. To reveal cell nuclei, the same slides were stained with 4',6-diamidino-2-phenylindole (DAPI; 1  $\mu$ g/ml) in phosphate-buffered saline (PBS) plus 0.5% 1,4-diazabicyclo [2,2,2] octane. Immunofluorescence images were obtained using a fluorescence microscope (Eclipse,



Nikon, Japan) equipped with a digital camera (DXM1200, Nikon). Cell surface areas were measured by morphometric analysis of  $\alpha$ -actinin-stained cardiomyocytes using NIH image software. Cell size was quantified by measuring cell surface area in randomly chosen cells from different dishes.

**Flow cytometric assay of 2',7'-dichlorodihydrofluorescein oxidation** The determination of intracellular ROS production was based on the oxidation of 2',7'-dichlorodihydrofluorescein (DCFH) to fluorescent 2',7'-dichlorofluorescein (DCF), as described previously (Chen et al., 2008). DCFH was added at a final concentration of 10  $\mu$ M and incubated for 30 min at 37°C. The cells were then washed once with PBS and maintained in a 1-ml culture medium. Following drug treatment, the medium was aspirated and cells were washed twice with PBS, and then dissociated with trypsin. Cellular fluorescence was determined by flow cytometry (FACS-SCAN, Becton-Dickinson, Franklin Lakes, NJ). Cells were excited with an argon laser at 488 nm, and measurements were taken at 510–540 nm.

**Western blot analysis** Rabbit polyclonal anti-phospho-ERK antibody and mouse monoclonal anti-phospho-EGFR (Tyr1068) antibody were purchased from New England Biolabs (Beverly, MA) and Cell Signaling Technology Inc. (Danvers, MA). Anti-ERK, anti-EGFR, anti-p47<sup>phox</sup>, anti-PTP1B, anti-SHP2 antibodies were purchased from Santa Cruz Biotechnology Inc (Santa Cruz, CA). Whole-cell extracts were obtained in a radioimmunoprecipitation assay buffer (10 mM Tris, pH 7.5, 150 mM NaCl, 0.1% sodium dodecyl sulfate, 1.0% Triton X-100, 1% sodium deoxycholate, 5 mM ethylenediaminetetraacetic acid, 1 mM sodium orthovanadate, 1 mM phenylmethanesulphonylfluoride, and protease inhibitor cocktail; Complete, Roche

Diagnostics GmbH, Germany). Extracts or proteins were separated by sodium dodecyl sulfate polyacrylamide gel electrophoresis followed by electrotransfer to polyvinylidene difluoride membranes and probed with antisera, followed by horseradish peroxidase-conjugated secondary antibodies. The proteins were visualized by chemiluminescence, according to the manufacturer's instructions (Pierce Biotechnology Inc., IL).

**Protein synthesis measurement ( $^3\text{H}$ -leucine incorporation)** To measure synthesis of new protein, cardiomyocytes were incubated with 1.0  $\mu\text{Ci}/\text{ml}$   $^3\text{H}$ -leucine in serum-free medium (Cheng et al., 2005b). Cells were harvested by incubation at 4 °C with trichloroacetic acid (5%) followed by solubilization in 0.1 N NaOH. Radioactivity was determined by scintillation counting.

**Immunoprecipitation** Cardiomyocyte cultures were starved overnight in serum-free culture medium and stimulated with or without 1 nM U-II at 37°C. The cells were lysed at 4°C in lysis buffer (50 mM Tris, pH 7.5, 1% Nonidet P-40, 0.5% sodium deoxycholate, 150 mM NaCl, protease inhibitors). Target proteins were collected using an immunoprecipitation kit (Roche Molecular Biochemicals, Germany) with specific antibodies and protein-G-agarose, according to the manufacturer's instructions.

**Detection of cysteine oxidation in phosphotyrosine phosphatases** The oxidation of the active site cysteine residue in PTPs was detected using a process described in our previous study (Chen et al., 2006). Treated rat cardiomyocytes were lysed at room temperature in a dark environment for 20 min in lysis buffer with 100 mM iodoacetic acid (IAA). PTPs were collected by immunoprecipitation with specific antibodies and protein-G-agarose beads. The beads were washed 3 times in lysis buffer, incubated with

10 mM dithiothreitol for 10 min on ice, washed again 3 times, and stored in distilled water. Phosphatase activity of the samples was detected by malachite green using the Tyrosine Phosphatase Assay Kit-1 (Upstate Biotechnology, NY), according to the manufacturer's instructions.

***siRNA-mediated gene knockdown and fluorescence observation of green fluorescent protein*** SHP-2 siRNA (sc-36489), p47<sup>phox</sup> siRNA (sc-36157), and control siRNA (sc-37007) were purchased from Santa Cruz Biotechnology, and used for SHP-2 knockdown, p47<sup>phox</sup> knockdown, and experimental control, respectively. Transfection of siRNA in cardiomyocytes was performed using siRNA transfection reagent, according to the manufacturer's instructions (Santa Cruz Biotechnology Inc.). Transfected cells were subsequently processed for western blot analysis and advanced assays. In a subset of experiments examining morphologic changes of cardiomyocytes, cotransfections of green fluorescent protein (GFP) expression plasmids (a gift from Prof. Jeremy Jan-Way Chen, Institute of Biomedical Sciences, National Chong-Hsin University, Taichung, Taiwan) and siRNAs were carried out at a ratio of 1:3 with Lipofectamine 2000 (Invitrogen), according to the manufacturer's instructions. Fluorescence of GFP in transfected cells was monitored by fluorescence microscopy (Eclipse, Nikon, Japan).

***Statistical analysis*** Results are expressed as mean  $\pm$  S.E.M. The number of experiments (n) is given in each figure legend. Statistical analysis was performed using Student's t test or analysis of variance (ANOVA), followed by a Dunnett multiple comparison test using GraphPad Prism (GraphPad Software, San Diego, CA). A value of  $P < 0.05$  was considered statistically significant.

## Results

***Roles of EGFR transactivation and ERK phosphorylation in U-II-induced cardiomyocyte hypertrophy*** To determine whether EGFR transactivation can be induced by U-II in rat cardiomyocytes, EGFR was immunoprecipitated using goat anti-EGFR antibody. As shown in Figure 1A, 0.5-10 nM U-II induced significant phosphorylation of EGFR. At a concentration of 0.5–1 nM, the effect of U-II on EGFR phosphorylation was maximal. Following treatment of 1 nM of U-II, EGFR phosphorylation was detected within 1 min (reaching a maximum at 2 min), and was sustained through 10 min of treatment (Fig. 1B). Extracellular signal-regulated kinases are important signaling molecules in the EGFR pathway. It was found phosphorylation of ERK also increased within 2 min of U-II exposure, which was sustained through 30 min of treatment (Fig. 1C). There was a pronounced increase in the size of cardiomyocytes treated with 1 nM U-II for 24 h, as well as a significant increase in protein synthesis of these cells relative to control-treated cells (Fig. 1, D, E, and F). These effects were reduced by pretreatment with EGFR inhibitor, AG1478 (100 nM), or 1,4-diamino-2,3-dicyano-1,4-bis(o-aminophenylmercapto)butadiene (U0126, a MEK kinase inhibitor; 1  $\mu$ M) for 30 min. These findings implicate EGFR transactivation and ERK phosphorylation in U-II-induced cardiomyocyte hypertrophy.

***Role of ROS generation in U-II-induced EGFR transactivation and cardiomyocyte hypertrophy*** It has been shown that U-II stimulates ROS generation in various cell types (Chen et al., 2008; Djordjevic et al., 2005). To determine the influence of ROS on EGFR transactivation in the U-II signaling pathway in cardiomyocytes, phosphorylation of EGFR induced by U-II was examined in

cardiomyocytes following treatment with the NAD(P)H oxidase inhibitor, apocynin, or the ROS scavenger *N*-acetylcysteine (NAC). As shown in Figure 2A, treatment with apocynin (0.5 mM), NAC (5 mM), or the EGFR inhibitor AG1478 resulted in decreased U-II-induced phosphorylation of EGFR. ERK showed a similar pattern of phosphorylation to EGFR when treated with NAC, apocynin, or AG1478 (Fig. 2B). U-II-induced cardiomyocyte hypertrophy, and [<sup>3</sup>H]leucine uptake was suppressed after pre-treatment with NAC and apocynin (Fig. 2, B, and C). These data suggest ROS are involved in EGFR transactivation and U-II-induced cardiomyocyte hypertrophy.

Levels of ROS were significantly increased compared to control cells after U-II challenge (Fig. 3). A flow cytometric histogram of DCF fluorescence in cardiomyocytes from a typical time-course experiment is shown in Figure 3A. Time-course experiments revealed that the addition of U-II (1 nM) to cardiomyocytes transiently induced ROS production, which peaked 2 min after stimulation and then declined (Fig. 3B). The addition of U-II (0.5–10 nM; 2 min) induced a significant increase in ROS production (Fig. 3C). We also examined the influence of EGFR transactivation on ROS generation caused by U-II. As shown in Figure 3D, U-II-induced ROS generation in rat cardiomyocytes was reduced by apocynin and NAC, but not AG1478. In addition, apocynin is an inhibitor of many flavoprotein enzymes but not specific to NADPH oxidase. To confirm the role of NADPH oxidase in U-II-induced ROS generation, NADPH oxidase subunit p47<sup>phox</sup> siRNAs were used for NADPH oxidase knockdown cells. As shown in Fig. 3E, the expression level of p47<sup>phox</sup> was significantly reduced in p47<sup>phox</sup> siRNA transfection cells compared with the mock controls. The U-II-induced ROS generation was also decreased apparently in siRNA transfection cells (Fig. 3F). These results

suggest ROS generation via NADPH oxidase is necessary for EGFR transactivation and subsequent myocyte hypertrophy in U-II-treated rat cardiomyocytes.

***Interactions between Src homology 2-containing tyrosine phosphatase and EGFR during U-II treatment*** In our previous study, we found that Src homology 2-containing tyrosine phosphatase (SHP-2) is involved in EGFR transactivation in the ET-1 signaling pathway (Chen et al., 2006). To further investigate the role of SHP-2 in U-II-induced EGFR transactivation, we examined the interaction between SHP-2 and EGFR in U-II-treated cardiomyocytes by co-immunoprecipitation. Time-course studies revealed that within 1 min, co-immunoprecipitated SHP-2 was significantly increased following treatment with 1 nM, after which dissociation occurred (Fig. 4A). In contrast, using the same experimental conditions, the tyrosine phosphatase PTP-1B was detected only at basal levels (Fig. 4B). As shown in Fig. 4C, we immunoprecipitated EGFR and found significant co-immunoprecipitation of SHP-2 following treatment with U-II at a concentration of 0.5–5 nM. However, U-II-mediated SHP-2 co-immunoprecipitation was significantly reduced by pre-treatment with NAC (5 mM; 30 min) (Fig. 4C). These results indicate that SHP-2 interacts with EGFR in U-II signaling pathways in cardiomyocytes, which may play an important role in regulation of EGFR transactivation.

***Transient oxidization of the SHP-2 cysteine residue in the U-II signaling pathway*** ROS are able to transiently inhibit PTPs through the reversible oxidization of the catalytic cysteine residue, thereby suppressing protein dephosphorylation (Meng et al., 2002). We examined oxidation of the catalytic cysteine residue in various PTPs to elucidate the role of SHP-2 in U-II-mediated signaling pathways. The data shown in Figure 5A illustrate oxidation of the catalytic cysteine residue of SHP-2 was significantly increased

at an early stage (within approximately 5 min) following U-II treatment. There was, however, no significant change in the oxidation of the catalytic cysteine of PTP-1B during U-II treatment (Fig. 5B). In other words, the active site cysteine residue of SHP-2 was oxidized, resulting in suppressed dephosphorylatory activity during the initial stage of U-II treatment, after which there was a rapid recovery. We further examined the influence of U-II-induced ROS on the oxidation of the catalytic cysteine residue of SHP-2 in rat cardiomyocytes treated with inhibitors. In each sample, SHP-2 was immunoprecipitated with anti-SHP-2 antibody, and subjected to the PTP cysteine oxidation detection procedure. As shown in Figure 5C, U-II induced oxidation of the catalytic cysteine residue in SHP-2, which was reversed by the addition of NAC or apocynin. However, the EGFR inhibitor AG1478 did not influence upon U-II-induced SHP-2 oxidation. These results suggest that U-II regulates the activity of SHP-2 *via* ROS generation, but not EGFR transactivation.

***Involvement of SHP-2 in U-II-induced EGFR transactivation and cardiomyocyte hypertrophy*** To further investigate the regulatory role of SHP-2 in U-II-induced EGFR transactivation, SHP-2 siRNA was used for SHP-2 knockdown in rat cardiomyocytes. Compared to experimental controls, SHP-2 siRNA (100 nM) significantly reduced SHP-2 expression in rat cardiomyocytes (Fig. 6A). As shown in Fig. 6B, basal phosphorylation levels of EGFR in SHP-2 knockdown cells were slightly higher than those in experimental control rat cardiomyocytes. Phosphorylation of EGFR induced by U-II was highly increased in SHP-2 knockdown cardiomyocytes. The ROS scavenger, NAC, did not reduce U-II-induced EGFR phosphorylation in SHP-2 siRNA-transfected cells, although it was associated with decreased EGFR phosphorylation in experimental

controls (Fig. 6B). Furthermore, after treatment with 1 nM U-II for 24 h, cardiomyocytes transfected with SHP-2 siRNA and GFP expression plasmid exhibited a pronounced increase in cell size (Fig. 6, C, and D), as well as a significant rise in protein synthesis relative to control-treated cells (Fig. 6E). Pre-treatment with NAC had no impact upon these effects. These results suggest ROS-mediated transient inhibition of SHP-2 is necessary for U-II-induced EGFR transactivation that underlies cardiomyocyte hypertrophy.



## Discussion

This study examined EGFRs as potential downstream effectors of U-II signaling leading to hypertrophy in neonatal rat cardiomyocytes. We found that ROS production and transient oxidation of Src homology 2-containing tyrosine phosphatase is involved in U-II-induced hypertrophy, ERK phosphorylation and EGFR transactivation in rat cardiomyocytes (Fig. 7). Tzanidis *et al.* (Tzanidis *et al.*, 2003) have demonstrated expression of both U-II and its corresponding receptor molecule within myocardial tissue, which suggests an important role for U-II in cardiac pathophysiology. To explore the potential role of U-II-related signaling in cardiac cell dysfunction, the effects of exogenous U-II on isolated cardiac cells were examined *in vitro*. In addition to its vasoconstrictive effect, we showed that exogenous U-II stimulates myocyte hypertrophy in rat cardiomyocytes. Similarly, Zou *et al.* (Zou *et al.*, 2001) reported U-II-dependent hypertrophic changes in isolated cardiomyocyte cultures. However, in contrast to our findings, Onan *et al.* (Onan *et al.*, 2004) reported that U-II does not exhibit an analogous hypertrophic stimulus in quiescent myocytes cultures. These apparently contradictory findings may be partly explained by differences in the preparation cardiomyocyte cultures. Further studies suggest expression levels of U-II receptors in neonatal cardiomyocytes are below the threshold necessary to support sustained signaling required for the hypertrophic response. Therefore, it appears U-II receptor levels must be optimally regulated to obtain myocyte hypertrophy following U-II stimulation.

In addition, we showed that U-II induces ERK phosphorylation in rat cardiomyocytes. Zou *et al.* have previously shown that U-II-induced cardiomyocyte hypertrophy is

associated with significant ERK activation (Zou et al., 2001). Hypertrophic activity, which involves several intracellular mechanisms including the ERK-dependent signaling pathway, has been demonstrated in response to other vasoactive peptides, such as angiotensin II (Cheng et al., 2004b) and endothelin-1 (Cheng et al., 2005a). The present results further implicate ROS involvement in U-II-induced myocyte hypertrophy, ERK phosphorylation and EGFR transactivation. Recent reports have shown that U-II stimulates membrane-bound NAD(P)H oxidase, which generates ROS in pulmonary artery smooth muscle cells (Djordjevic et al., 2005). The recent research suggested that endothelin-1-mediated ROS generation can transiently inhibit SHP-2 activity to facilitate the HB-EGF-stimulated EGFR transactivation in rat cardiac fibroblasts (Chen et al., 2006). Inspired by the endothelin-1 study, we investigated the molecular mechanisms by which U-II activates mitogenic signaling pathways, and also found that U-II-stimulated ROS generation can induce EGFR transactivation via transient inhibition of SHP-2 in cardiomyocytes. This mechanism enables EGFR to transmit signals to the downstream mitogenic signaling pathway, and may extensively exist in G protein-coupled receptors-mediated EGFR transactivation. In this study, we showed that U-II can induce tyrosine phosphorylation of EGFR in rat cardiomyocytes. In our time-course experiments, U-II first induced transactivation of EGFR and induced ERK activation thereafter. Moreover, blockade of EGFR activation by AG1478 significantly reduced ERK phosphorylation. This is likely to cause phosphorylated EGFR to biochemically interact with SHP-2, resulting in EGFR dephosphorylation. U-II induces ROS generation, which may lead to transient oxidation of the catalytic cysteine residue of SHP-2, thereby suppressing its dephosphorylatory activity. EGFR has been implicated in ERK activation

induced by various ligands, such as endothelin-1 (Chen et al., 2006), leptin (Chao et al., 2007), and U-II (Chen et al., 2008). Our results are consistent with previous reports (Onan et al., 2004), and suggest that in various signaling pathways induced by U-II, EGFR transactivation acts upstream of ERK signaling pathways.

In this study, at a concentration of 0.5–1 nM, the effect of U-II on EGFR phosphorylation was maximal. One reason for the observed atypical dose-response curve could be the low receptor density of the investigated cardiomyocytes (Tzanidis et al., 2003). However, the detailed mechanism still remains to be determined. In addition, we demonstrated an association between ROS and EGFR transactivation *via* the transient inhibition of PTPs through the reversible oxidation of catalytic cysteine residues (which suppresses protein dephosphorylation) (Meng et al., 2002). Using a modified malachite green-PTP activity assay, we found that the catalytic cysteine residue of SHP-2, a PTP, was significantly oxidized at an early stage after U-II treatment. The biological interaction between SHP-2 and EGFR was also revealed through co-immunoprecipitation. U-II-induced EGFR phosphorylation was dramatically elevated in SHP-2 knockdown cells, and this was not suppressed by NAC. These results reveal that SHP-2 is a potent mediator in U-II-induced transactivation of EGFR. In contrast, another oxidation-sensitive PTP, PTP-1B, does not interact with EGFR and is not oxidized following activation of the U-II signaling pathway, although transient oxidation of PTP-1B is known to play a crucial role in insulin signaling (Meng et al., 2004). In SHP-2 knockdown cells, U-II-induced phosphorylation of EGFR was dramatically elevated. This elevation was not suppressed by NAC (Fig. 6B). Therefore, SHP-2 plays a specific role in the biological mechanism that links EGFR transactivation to ROS generation in the

## U-II signaling pathway.

As has been previously described for other vasoconstrictor peptides such as angiotensin II (Cheng et al., 2004) and endothelin-1 (Cheng et al., 2005a), myocyte hypertrophy induced by U-II, may similarly contribute to cardiac remodeling and deterioration in systolic and diastolic function. These chronic effects have classically been considered as the key mechanisms through which neurohumoral agents influence the diastolic properties of the myocardium. Further studies are required for understanding the relevance of our findings in relation to human cardiovascular pathology. It is attractive to speculate that these results may be important in terms of understanding the potential role of U-II in cardiac dysfunction and cardiac diseases. In summary, the data presented here reveal that ROS generation is essential for EGFR transactivation in U-II-mediated signaling mechanisms. In rat cardiomyocytes, increased levels of ROS specifically inhibit SHP-2 activity at an early stage following U-II treatment, which facilitates a transient increase in phosphorylation of EGFR. After activation of the EGFR signaling pathway, U-II can induce phosphorylation of ERK to promote the hypertrophy of rat cardiomyocytes. In other words, ROS generation is involved in EGFR transactivation through the transient oxidation of SHP-2 in the U-II-induced hypertrophy signaling pathway in rat cardiomyocytes.

## **Acknowledgements**

This study was presented in a preliminary format at "The 72<sup>nd</sup> Annual Scientific Meeting of the Japanese Circulation Society", Fukuoka, Japan, 2008.

## References

- Bousette N and Giaid A (2006) Urotensin-II and cardiovascular diseases. *Curr Hypertens Rep* **8**(6):479-483.
- Chao HH, Hong HJ, Liu JC, Lin JW, Chen YL, Chiu WT, Wu CH, Shyu KG and Cheng TH (2007) Leptin stimulates endothelin-1 expression via extracellular signal-regulated kinase by epidermal growth factor receptor transactivation in rat aortic smooth muscle cells. *Eur J Pharmacol* **573**(1-3):49-54.
- Chen CH, Cheng TH, Lin H, Shih NL, Chen YL, Chen YS, Cheng CF, Lian WS, Meng TC, Chiu WT and Chen JJ (2006) Reactive oxygen species generation is involved in epidermal growth factor receptor transactivation through the transient oxidization of Src homology 2-containing tyrosine phosphatase in endothelin-1 signaling pathway in rat cardiac fibroblasts. *Mol Pharmacol* **69**(4):1347-1355.
- Chen YL, Liu JC, Loh SH, Chen CH, Hong CY, Chen JJ, Cheng TH. (2008) Involvement of reactive oxygen species in urotensin II-induced proliferation of cardiac fibroblasts. *Eur J Pharmacol* **593**(1-3):24-29.
- Cheng TH, Liu JC, Lin H, Shih NL, Chen YL, Huang MT, Chan P, Cheng CF and Chen JJ (2004) Inhibitory effect of resveratrol on angiotensin II-induced cardiomyocyte hypertrophy. *Naunyn Schmiedeberg's Arch Pharmacol* **369**(2):239-244.
- Cheng TH, Shih NL, Chen CH, Lin H, Liu JC, Chao HH, Liou JY, Chen YL, Tsai HW, Chen YS, Cheng CF and Chen JJ (2005a) Role of mitogen-activated protein kinase pathway in reactive oxygen species-mediated endothelin-1-induced beta-myosin heavy chain gene expression and cardiomyocyte hypertrophy. *J Biomed Sci* **12**(1):123-133.

- Cheng TH, Shih NL, Chen SY, Lin JW, Chen YL, Chen CH, Lin H, Cheng CF, Chiu WT, Wang DL and Chen JJ (2005b) Nitric oxide inhibits endothelin-1-induced cardiomyocyte hypertrophy through cGMP-mediated suppression of extracellular-signal regulated kinase phosphorylation. *Mol Pharmacol* **68**(4):1183-1192.
- Cheng TH, Shih NL, Chen SY, Wang DL and Chen JJ (1999) Reactive oxygen species modulate endothelin-I-induced c-fos gene expression in cardiomyocytes. *Cardiovasc Res* **41**(3):654-662.
- Djordjevic T, BelAiba RS, Bonello S, Pfeilschifter J, Hess J and Gorlach A (2005) Human urotensin II is a novel activator of NADPH oxidase in human pulmonary artery smooth muscle cells. *Arterioscler Thromb Vasc Biol* **25**(3):519-525.
- Liebmman C and Bohmer FD (2000) Signal transduction pathways of G protein-coupled receptors and their cross-talk with receptor tyrosine kinases: lessons from bradykinin signaling. *Curr Med Chem* **7**(9):911-943.
- Matsushita M, Shichiri M, Fukai N, Ozawa N, Yoshimoto T, Takasu N and Hirata Y (2003) Urotensin II is an autocrine/paracrine growth factor for the porcine renal epithelial cell line, LLCPK1. *Endocrinology* **144**(5):1825-1831.
- Meng TC, Buckley DA, Galic S, Tiganis T and Tonks NK (2004) Regulation of insulin signaling through reversible oxidation of the protein-tyrosine phosphatases TC45 and PTP1B. *J Biol Chem* **279**(36):37716-37725.
- Meng TC, Fukada T and Tonks NK (2002) Reversible oxidation and inactivation of protein tyrosine phosphatases in vivo. *Mol Cell* **9**(2):387-399.
- Ni YG, Berenji K, Wang N, Oh M, Sachan N, Dey A, Cheng J, Lu G, Morris DJ, Castrillon

- DH, Gerard RD, Rothermel BA and Hill JA (2006) Foxo transcription factors blunt cardiac hypertrophy by inhibiting calcineurin signaling. *Circulation* **114**(11):1159-1168.
- Onan D, Pipolo L, Yang E, Hannan RD and Thomas WG (2004) Urotensin II promotes hypertrophy of cardiac myocytes via mitogen-activated protein kinases. *Mol Endocrinol* **18**(9):2344-2354.
- Papadopoulos P, Bousette N and Giaid A (2008) Urotensin-II and cardiovascular remodeling. *Peptides* **29**(5):764-769.
- Saffitz JE, Hames KY and Kanno S (2007) Remodeling of gap junctions in ischemic and nonischemic forms of heart disease. *J Membr Biol* **218**(1-3):65-71.
- Tzanidis A, Hannan RD, Thomas WG, Onan D, Autelitano DJ, See F, Kelly DJ, Gilbert RE and Krum H (2003) Direct actions of urotensin II on the heart: implications for cardiac fibrosis and hypertrophy. *Circ Res* **93**(3):246-253.
- Zhang YG, Li YG, Liu BG, Wei RH, Wang DM, Tan XR, Bu DF, Pang YZ and Tang CS (2007) Urotensin II accelerates cardiac fibrosis and hypertrophy of rats induced by isoproterenol. *Acta Pharmacol Sin* **28**(1):36-43.
- Zou Y, Nagai R and Yamazaki T (2001) Urotensin II induces hypertrophic responses in cultured cardiomyocytes from neonatal rats. *FEBS Lett* **508**(1):57-60.



## Footnotes

This work was supported by the National Science Council [Grant NSC 95-2314-B-039-048-MY2], the New Century Health Care Promotion Foundation Medical Research Award [Grant 97-TMU-IAC-021], and the China Medical University [Grant CMU97-233], Taiwan, R.O.C.

### Legends for Figures

Fig. 1. Role of the induction of EGFR and ERK phosphorylation in U-II-induced cardiomyocyte hypertrophy. Data were expressed as percentage of control. *White bars* control (Cont), *black bars* treatment as indicated. \* $P < 0.05$  versus control; # $P < 0.05$  versus U-II alone. (A) Rat cardiomyocytes were treated with different concentration of U-II for 2 min; or 1 nM U-II for different time duration (B, and C). EGFR and phosphorylated EGFR were detected using western blotting with anti-EGFR and anti-phosphorylated EGFR (Tyr 1068) antibodies respectively. Anti-ERK and anti-phosphorylated ERK antibodies were used to detect ERK and phosphorylated ERK respectively. Densitometric analyses were performed with a densitometer. Results were shown as mean  $\pm$  S.E.M. (n=4). (D) U-II-induced morphologic changes of cardiomyocytes. Cultured cardiomyocytes were exposed to vehicle control (Cont; top left panel); or to U-II at 1 nM for 24 h in the absence (U-II; top right panel) or the presence of the EGFR inhibitor, AG1478 (U-II+AG1478; bottom left panel) or MEK inhibitor, U0126 (U-II+U0126; bottom right panel), and then immunostained with an anti- $\alpha$ -actinin antibody (red), and the nucleus was stained with DAPI (blue). Representative stained preparation from three independent experiments are shown. All images were taken at 100xmagnification. (E) Relative cardiomyocyte size. Cultured cardiomyocytes were exposed to vehicle control; or to U-II at 1 nM for 24 h in the absence or the presence of AG1478 or U0126. Surface area of cardiomyocytes was measured by using NIH Image software in 60 randomly chosen cells from three different dishes. Data are presented as mean  $\pm$  S.E.M. (F) Measurement of protein synthesis by using [ $^3$ H]leucine incorporation. Results were shown as mean  $\pm$  S.E.M. (n=4).

Fig. 2. Effects of antioxidants on U-II-induced cardiomyocyte hypertrophy. Cultured

cardiomyocytes were pretreated with 100 nM AG1478, 5 mM NAC, or 0.5 mM apocynin for 30 min; and then exposed to U-II at 1 nM for the time as indicated. Data were expressed as percentage of control. *White bars* control (Cont), *black bars* treatment as indicated. \* $P < 0.05$  versus control; # $P < 0.05$  versus U-II alone. (A) The western blotting of phospho-EGFR. The pretreated cells were then treated with 1 nM U-II for 2 min. Results were shown as mean  $\pm$  S.E.M. (n=4). (B) The western blotting of phospho-ERK. The pretreated cells were then treated with 1 nM U-II for 30 min. Results were shown as mean  $\pm$  S.E.M. (n=4). (C) Cardiomyocytes were pretreated with NAC or apocynin, and then treated with 1 nM U-II for 24 h, and relative cardiomyocyte size was measured in 60 randomly chosen cells from three different dishes. Results were shown as mean  $\pm$  S.E.M. (D) Cardiomyocytes were pretreated with NAC or apocynin, and then treated with 1 nM U-II for 24 h, and [ $^3\text{H}$ ]leucine incorporation was assayed. Results were shown as mean  $\pm$  S.E.M. (n=4).

Fig. 3. U-II-induced ROS generation in rat cardiomyocytes. Relative fluorescence intensity in rat cardiomyocytes was quantified by flow cytometry using DCFH-DA. Data were expressed as percentage of control. *White bars* control (Cont), *black bars* treatment as indicated. Results were shown as mean  $\pm$  S.E.M. (n=6) \* $P < 0.05$  versus control; # $P < 0.05$  versus U-II alone. (A) Flow cytometric histogram of DCF in cardiomyocytes. Cardiomyocytes were treated with vehicle control or U-II (1 nM) for different intervals (2, 5, 10, 15, and 30 min). Counts: cell number; FL1-H: relative DCF fluorescence intensity. (B) Column bar graph of mean cell fluorescence for DCF evaluated for different intervals (2, 5, 10, 15, and 30 min) after U-II (1 nM) treatments. The fluorescence intensities in untreated control cells are expressed as 100%. (C)

Column bar graph of mean cell fluorescence for DCF evaluated after U-II (0.5-50 nM) treatments for 2 min. (D) Cells were incubated with 10  $\mu$ M H<sub>2</sub>O<sub>2</sub>, 5 mM NAC, 0.5 mM apocynin, or 100 nM AG1478,. Except for the sample treated with H<sub>2</sub>O<sub>2</sub>, all samples were then treated with 1 nM U-II for 2 min. (E) Western blots of p47<sup>phox</sup> in p47<sup>phox</sup> knockdown cardiomyocytes. Control siRNA and p47<sup>phox</sup> siRNA (10 or 100 nM) were used for mock control and p47<sup>phox</sup> siRNA knockdown, respectively. Proteins from cardiomyocytes without treatment (Cont) or with control siRNA (M) or p47<sup>phox</sup> siRNA (sip47) transfection were detected by using polyclonal goat anti-p47<sup>phox</sup> antibody. GAPDH was used as a loading control. (F) U-II-induced ROS generation in p47<sup>phox</sup> knockdown cells. Rat cardiomyocytes with control siRNA (M) or p47<sup>phox</sup> siRNA (sip47, 100 nM) transfection were then treated with 1 nM U-II for 2 min.

Fig. 4. The association of EGFR with SHP-2. Rat cardiomyocytes were treated with 1 nM U-II for different time duration. Data were expressed as percentage of control. *White bars* control (Cont), *black bars* treatment as indicated. Results were shown as mean  $\pm$  S.E.M. (n=4). \**P*<0.05 versus control; #*P*<0.05 versus U-II alone. (A) EGFR of each sample was immunoprecipitated with goat anti-EGFR antibody. Co-immunoprecipitated SHP-2 was detected by Western blotting. (B) EGFR of each sample was immunoprecipitated with goat anti-EGFR antibody. Co-immunoprecipitated PTP-1B was detected by Western blotting. (C) Rat cardiomyocytes were treated with 5 mM NAC in the absence or the presence of different concentration of U-II for 1 min. EGFR of each sample was immunoprecipitated with goat anti-EGFR antibody. Co-immunoprecipitated SHP-2 was detected by Western blotting.

Fig. 5. Detection of the oxidization levels of SHP-2 and PTP-1B in U-II-treated

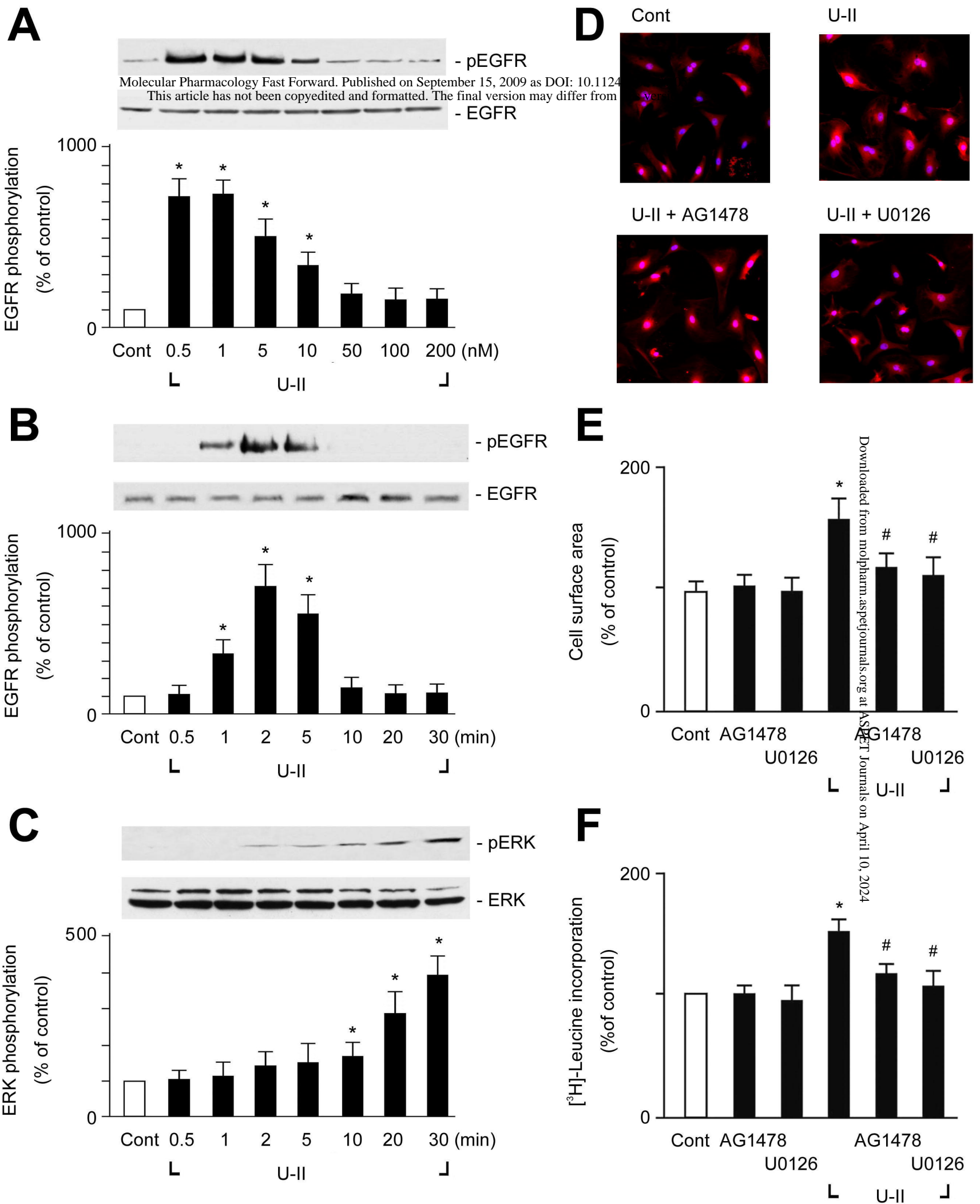
cardiomyocytes. Rat cardiomyocytes were treated with 1 nM U-II for different time duration, and then treated with IAA to block catalytic residues of protein tyrosine phosphatases. (A) SHP-2; and (B) PTP-1B in U-II treated cells were immunoprecipitated with rabbit anti-SHP-2 and anti-PTP-1B antibody respectively. (C) Effects of AG1478, NAC and apocynin on the SHP-2 oxidization in U-II-treated cells. Cardiomyocytes were pretreated with 100 nM AG1478, 5 mM NAC, or 0.5 mM apocynin for 30 min, respectively. All samples were treated with 1 nM U-II 2 min, and then treated with IAA. SHP-2 in rat cardiomyocytes was immunoprecipitated with rabbit anti-SHP-2 antibody, and applied in PTP cysteine oxidation detection. Purified SHP-2 or PTP-1B was then applied in Modified Malachite Green-PTP Assay. The relative oxidation levels of PTPs were recorded by measuring the relative increase in folds of liberated phosphate. Results were shown as mean  $\pm$  S.E.M. (n=6). \* $P$ <0.05 versus control; # $P$ <0.05 versus U-II alone.

Fig. 6. Phosphorylation patterns of EGFR induced by U-II in SHP-2 knockdown cardiomyocytes. (A) The effect of SHP-2 siRNA transfection on SHP-2 protein levels in cardiomyocytes. The cells were transfected with SHP-2 siRNA (si-SHP-2; 10 or 100 nM) to get SHP-2 knockdown cells. Control siRNA was also applied as mock controls (M). Western blotting was carried out with the specific antibody against SHP-2. GAPDH was used as a loading control. Results were shown in mean  $\pm$  S.E.M. (n = 3). \* $P$ <0.05 versus mock control. (B) Cardiomyocytes were either transfected with control siRNA as mock controls (M) or transfected with SHP-2 siRNA (si-SHP-2; 100 nM) to obtain SHP-2 knockdown cells. SHP-2 expression was determined using anti-SHP-2 antibodies. Cells were treated with 1 nM U-II for 2 min. To block U-II induced ROS generation, cells were

preincubated for 30 min at 37 °C with NAC before incubation with U-II. EGFR and phosphorylated EGFR were detected by using western blotting with anti-EGFR and pEGFR antibodies respectively. Results were shown in mean  $\pm$  S.E.M. ( $n = 4$ ).  $*P < 0.05$  versus mock control;  $^{\#}P < 0.05$  versus mock control with U-II treatment. (C) Cardiomyocytes were either cotransfected with control siRNA and GFP plasmid (M) or cotransfected with SHP-2 siRNA with GFP plasmid (si-SHP-2), and then treated with 1 nM U-II for 24 h in the absence or the presence of NAC, and then immunostained with an anti- $\alpha$ -actinin antibody (red); green color denoted the expression of GFP, and the nucleus was stained with DAPI (blue). Representative stained preparation from three independent experiments are shown. Top panels: left- cotransfected with control siRNA and GFP plasmid (M); right- cotransfected with SHP-2 siRNA and GFP plasmid, and then treated with 1 nM U-II for 24 h (si-SHP-2 + U-II). Middle panels: left- cotransfected with SHP-2 siRNA and GFP plasmid (si-SHP-2); right- cotransfected with control siRNA and GFP plasmid, and then treated with 1 nM U-II for 24 h in the presence of NAC (M + U-II + NAC). Bottom panels: left- cotransfected with control siRNA and GFP plasmid, and then treated with 1 nM U-II for 24 h (M + U-II); right- cotransfected with SHP-2 siRNA and GFP plasmid, and then treated with 1 nM U-II for 24 h in the presence of NAC (si-SHP-2 + U-II + NAC). All images were taken at 200xmagnification. (D) Cardiomyocytes were either cotransfected with control siRNA and GFP plasmid (M) or cotransfected with SHP-2 siRNA with GFP plasmid (si-SHP-2), and then treated with 1 nM U-II for 24 h in the absence or the presence of NAC, surface area of cardiomyocytes was measured in 20 randomly chosen cells from three different dishes. Data are presented as mean  $\pm$  S.E.M. (F) Cardiomyocytes were either transfected with control siRNA as mock controls

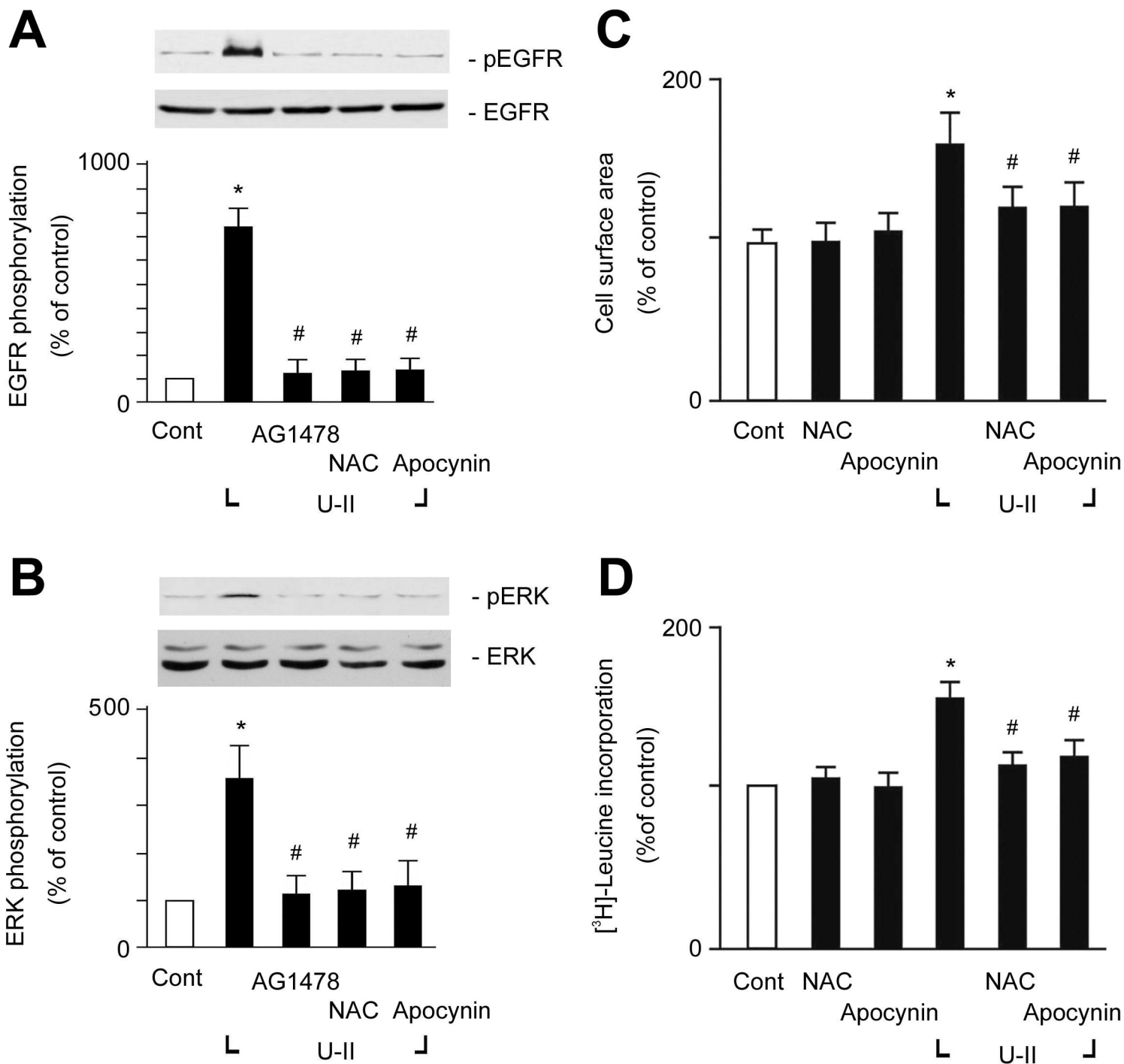
(M) or transfected with SHP-2 siRNA, and were pretreated with NAC, and then treated with 1 nM U-II for 24 h. Protein synthesis was measured by using [<sup>3</sup>H]leucine incorporation. Results were shown as mean  $\pm$  S.E.M. (n=4).

Fig. 7. Proposed molecular mechanism of the regulatory role of SHP-2 in U-II-induced EGFR transactivation in rat cardiomyocytes. The phosphorylated EGFR is associated with SHP-2 and is dephosphorylated. The U-II treatment induces ROS generation concomitantly *via* U-II receptors and NADPH oxidases; and causes the transient oxidization of catalytic cysteine of SHP-2 to inhibit the dephosphorylation activity of SHP-2. This mechanism allows transactivated EGFR to transmit signals to the downstream hypertrophic signaling pathway.

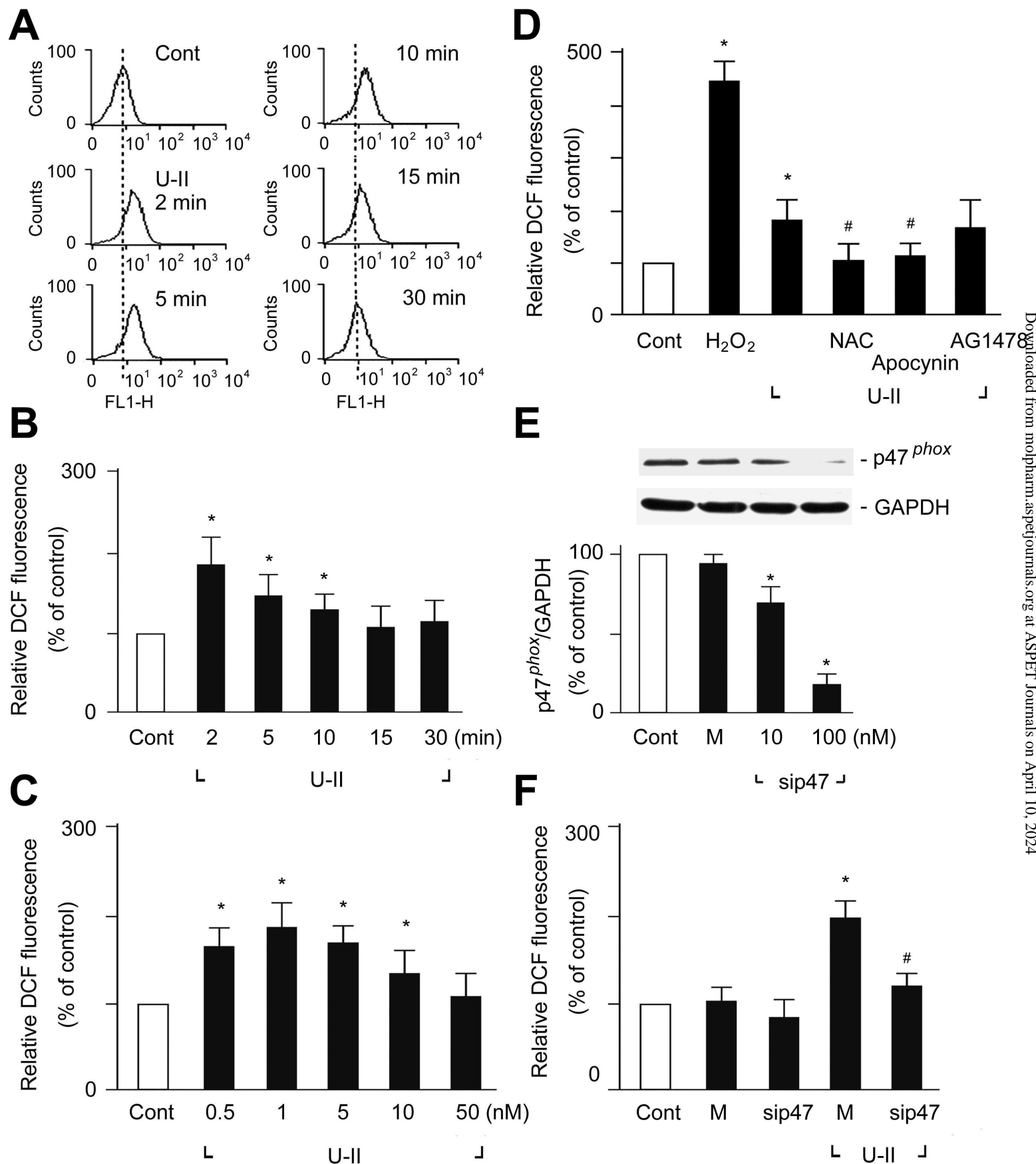


**Fig. 1**

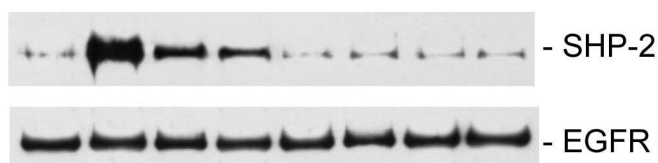




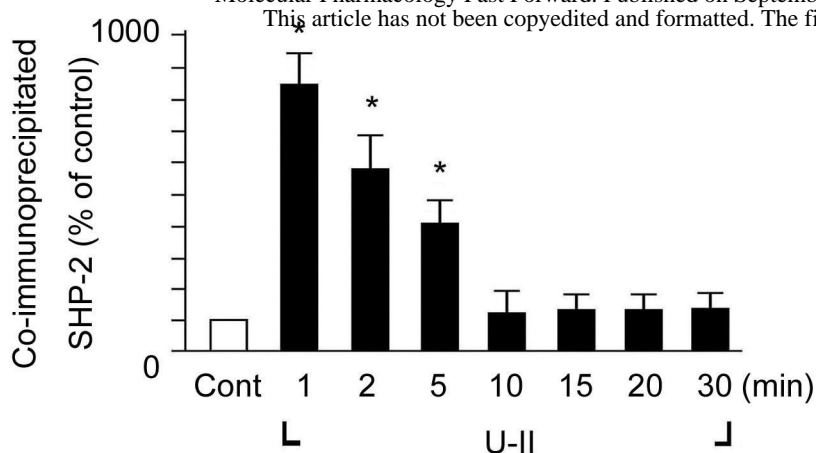
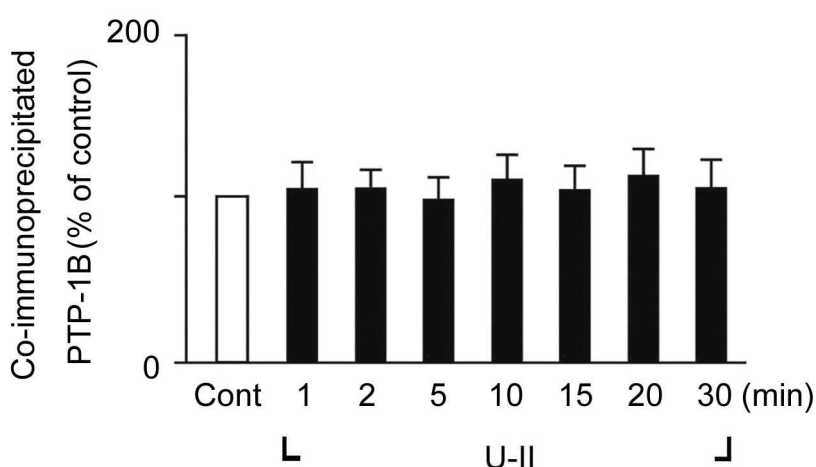
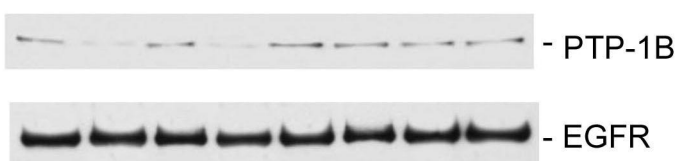
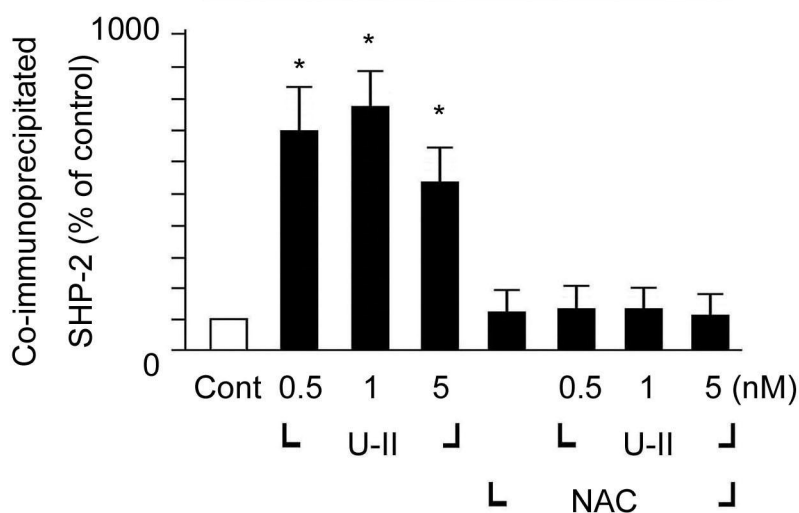
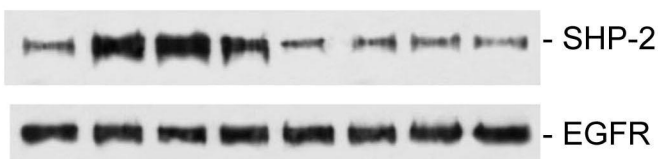
**Fig.2**

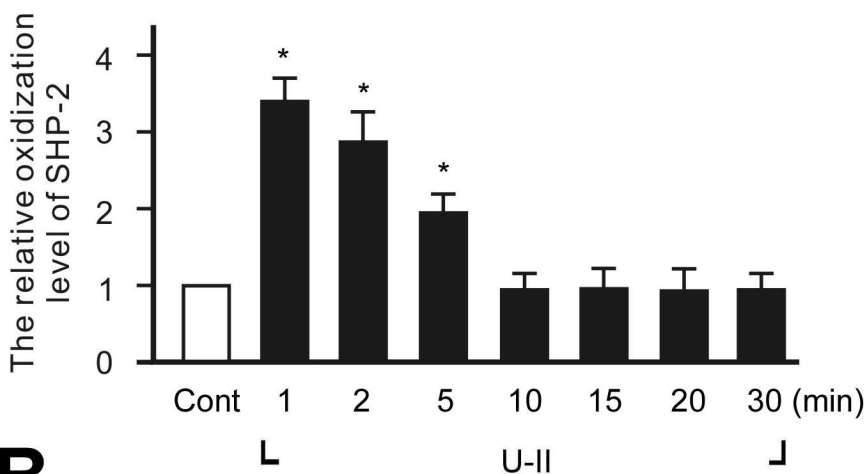
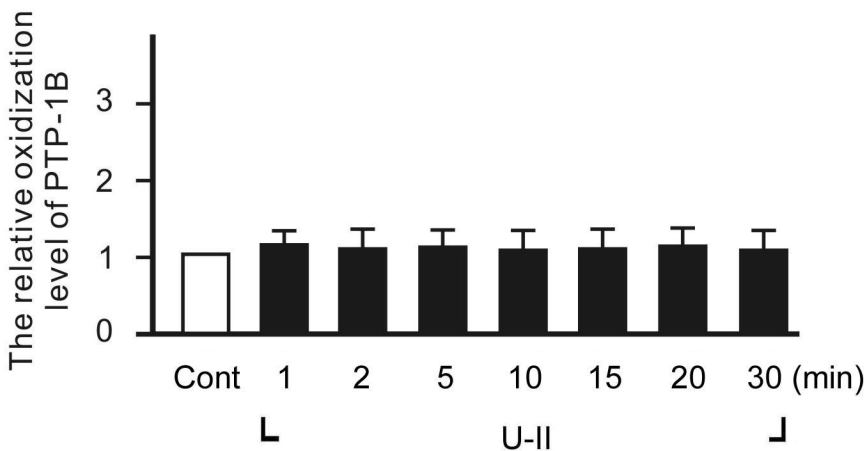
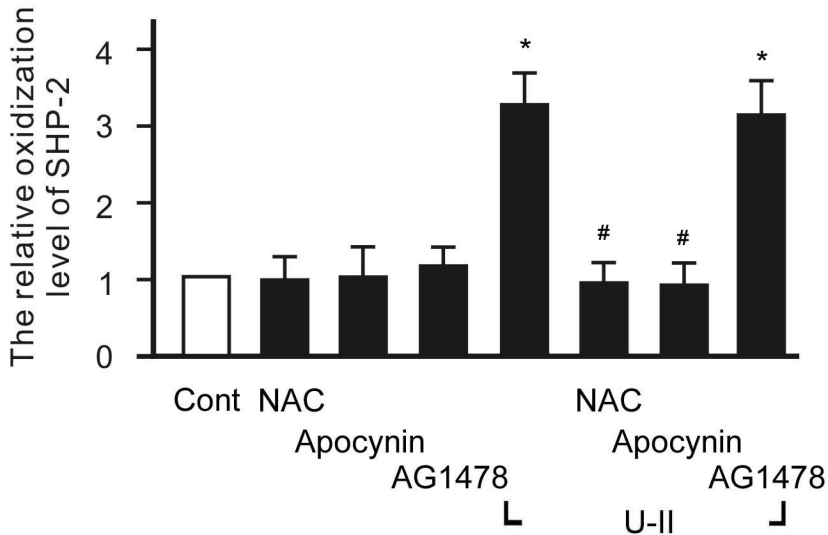


**Fig. 3**

**A**

Molecular Pharmacology Fast Forward. Published on September 15, 2009 as D  
This article has not been copyedited and formatted. The final version may

**B****C****Fig. 4**

**A****B****C****Fig. 5**

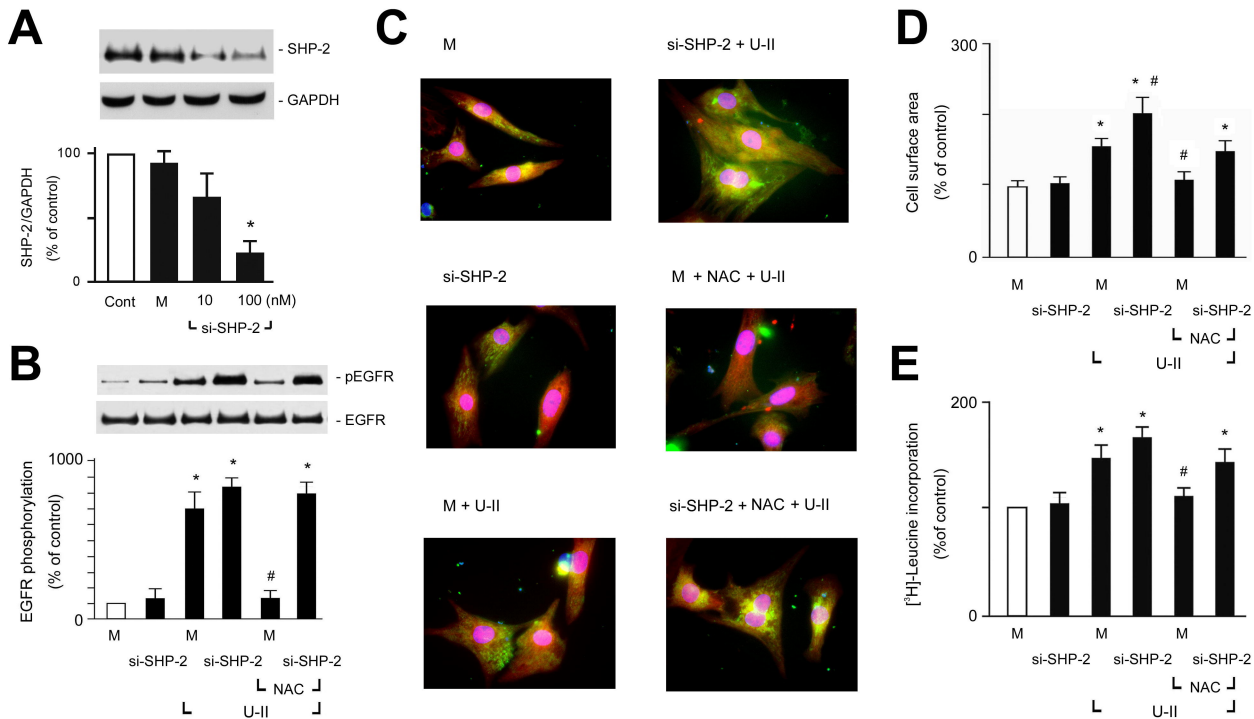


**Fig. 6**

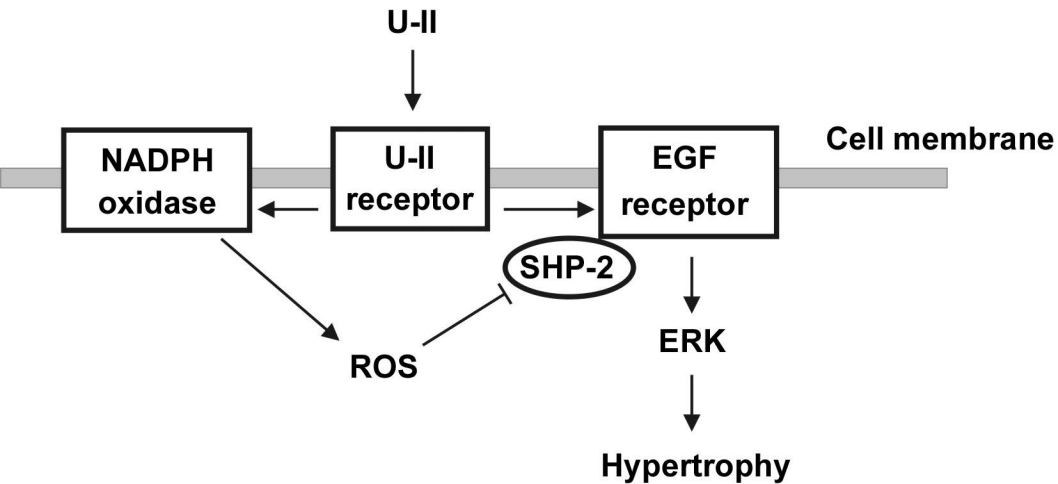


**Fig. 7**